

# A TRANSPORT EQUATION THEORY OF ELECTRON BACKSCATTERING AND X-RAY PRODUCTION

D. J. Fathers\* and P. Rez†

\*Department of Metallurgy and Science of Materials,  
University of Oxford, Oxford OX1 3PH, ENGLAND

†Department of Materials Science and Engineering  
University of California, Berkeley, California 94720

NOTICE  
 This report was prepared for the Office of Naval Research, Division of Materials Research, Naval Weapons Division, under the terms of a contract with the Office of Naval Research, Division of Materials Research, Naval Weapons Division, Department of the Navy, Arlington Hall Station, Arlington, Virginia. The views and conclusions contained herein are those of the author and do not necessarily represent those of the Office of Naval Research, Division of Materials Research, Naval Weapons Division, Department of the Navy, Arlington Hall Station, Arlington, Virginia.

To calculate the rate of x-ray production or backscattering a knowledge of the distribution of electrons in depth and velocity is needed. The behavior of the electron distribution function (the probability of finding an electron at a given point with a given velocity) is governed by the Boltzmann transport equation

$$\frac{\partial f}{\partial t} + \underline{v} \cdot \text{grad } f = \iiint v' \sigma(\underline{v}', \underline{v}) f(\underline{v}', \underline{r}', t) - v \sigma(\underline{v}, \underline{v}') f(\underline{v}, \underline{r}, t) d\underline{v}' \quad (1)$$

where  $\sigma(\underline{v}', \underline{v})$  is the probability per unit distance of an electron with initial velocity  $\underline{v}'$  being scattered to a final velocity  $\underline{v}$ . Rather than solve this integro-differential equation directly the usual approach has been to simulate the behavior of many electron trajectories by Monte-Carlo methods (see for example Shimizu, et al. [1]). The transport equation can be simplified by assuming solutions are stationary with respect to time and that the electron beam has infinite extent in the x,y plane (parallel to the specimen surface). Integrating over the azimuthal angle removes it from the equation as the cross section is a function of the difference in azimuthal angles of the incident and scattered states. Dependence on it can easily be calculated by Fourier transformation with respect to this variable. It is also convenient to rewrite the equation in terms of fluxes which can easily be related to observed currents

$$I(\theta, E, z) = v f(\theta, E, z) \quad 2.$$

$$\cos\theta \frac{dI}{dz}(\theta, E, z) = \int_0^\pi \int_0^{E_0} [\sigma(\theta, E; \theta', E') I(\theta', E', z) \left(\frac{E}{E'}\right)^{1/2} - \sigma(\theta, E'; \theta, E) I(\theta, E, z)] \sin\theta' d\theta' dE' \quad 3.$$

In many treatments further approximations are made at this stage. Bethe et al. [2] derive the corresponding Fokker-Plank equation and this has been solved by Brown, et al. [3] numerically using a grid in angle, depth, and integrated path length. It is also usual to expand in Legendre polynomials [4], [5], [6], but applying the boundary conditions is not easy and sometimes only spatial moments in an infinite foil with a source at the center were calculated [4], [5]. Integrated path length was nearly always used instead of energy to describe the electron state and this means that energy distributions were calculated assuming a continuous loss law. This has also been a problem with earlier Monte Carlo calculations [7].

Equation 3 is put into a matrix form by segmenting the angle and energy variables

$$\frac{dI_m^i}{dz} = \sum_j A_m^{ij} I_m^j + \sum_{nj} C_{mn}^{ij} I_n^j \quad 4.$$

where

$$I_m^i = I(\theta_i, E_m, z) \quad 5(a)$$

$$A_m^{ij} = \sigma(\theta_i, E_m; \theta_j, E_n) \sin\theta_j \sec\theta_i \Delta\theta\Delta E \quad i \neq j$$

$$A_m^{ii} = (\sigma(\theta_i, E_m; \theta_i, E_m) - \sum_{nj} \sigma(\theta_j, E_n; \theta_i, E_m)) \sin\theta_i \sec\theta_i \Delta\theta\Delta E \quad 5(b)$$

$$C_{mn}^{ij} = \sigma(\theta_i, E_m; \theta_j, E_n) \sin\theta_j \sec\theta_i \quad 5(c)$$

Dashen [8] uses a similar approach but derives a nonlinear equation for the matrix relating forward and backward traveling fluxes. As electrons only lose energy and it is also a good approximation to assume that they are only scattered

from one energy level to the next equation 4 can be rewritten as a coupled supermatrix differential equation. The diagonal matrixes represent the elastic scattering and the "absorption" due to inelastic scattering and those on the next lower off diagonal represent the coupling between the energy states due to inelastic scattering

$$\frac{d}{dz} \begin{pmatrix} I_0 \\ I_1 \\ I_2 \\ \vdots \end{pmatrix} = \begin{pmatrix} A_0 & 0 & 0 & \dots \\ C_{10} & A_1 & 0 & \dots \\ 0 & C_{21} & A_2 & \dots \\ \vdots & \vdots & \vdots & \ddots \end{pmatrix} \begin{pmatrix} I_0 \\ I_1 \\ I_2 \\ \vdots \end{pmatrix} \quad 6.$$

A further simplification is to assume only one energy loss equal to the incident energy and this means that absorption from the incident state is the only effect of the inelastic scattering. The resulting matrix differential equation has a simple solution

$$I(t) = \exp At I(0) \quad 7.$$

which can be evaluated by diagonalizing the matrix. As there is a symmetry between forward and backward scattering before applying the boundary conditions the eigenvalues and eigenvectors can be partitioned

$$\begin{pmatrix} I_F(t) \\ I_B(t) \end{pmatrix} = \begin{pmatrix} V1 & V2 \\ V2 & V1 \end{pmatrix} \begin{pmatrix} \exp \lambda t & 0 \\ 0 & \exp -\lambda t \end{pmatrix} \begin{pmatrix} V1 & V2 \\ V2 & V1 \end{pmatrix}^{-1} \begin{pmatrix} I_F(0) \\ I_B(0) \end{pmatrix} \quad 8.$$

This can be solved for  $I_B(0)$ ,  $I_F(t)$  subject to the boundary conditions  $I_F(0) = \delta_{i,i_0}$ ,  $I_B(t) = 0$  and gives

$$I_F(t) = (V2 - V1V2^{-1}V1) \exp -\lambda t V2^{-1} (I + V1 \exp -\lambda t V2^{-1} V1 \exp -\lambda t V2^{-1}) \quad 9(a).$$

$$I_B(t) = (V1V2^{-1} - V2 \exp -\lambda t V2^{-1} V1 \exp -\lambda t V2^{-1}) (I + V1 \exp -\lambda t V2^{-1} V1 \exp -\lambda t V2^{-1}) \quad 9(b).$$

As can be seen if  $t$  tends to infinity the backscattered flux becomes

$$I_B(0) = V1V2^{-1} I_F(0) \quad 10.$$

and this is the solution matrix of Dashen's nonlinear equation. The forward and backward traveling fluxes at depth  $z$  are:

$$I_F(z) = V_2 \exp(-\lambda z) V_2^{-1} I_F(0), \quad I_B(z) = V_1 \exp(-\lambda z) V_2^{-1} I_F(0) \quad 11.$$

The solution for the supermatrix differential equation (6) where many energy levels are considered proceeds in a similar way. The supermatrix is diagonalized in two stages. The first step is to bring it to a block diagonal form analogous to an eigenvalue matrix with the matrices  $A^m$  along the diagonal. This can be done by solving matrix commutator equations involving these matrices by diagonalization. The supermatrix eigenvalues and eigenvectors are found by expressing the diagonal matrices  $A^m$  in terms of their eigenvalues and eigenvectors and a numerical procedure was devised where the solution for each energy is found using the eigenvector elements of the previous energy. The time taken to diagonalize the supermatrix by this method is proportional to the number of energy levels. The partitioning can then be done and the solution is similar to that given previously except that the matrices now have indices corresponding to energy. The backscattering at energy  $i$  is given by

$$I_E^i(0) = \sum_j V_{1ij} V_{2j0}^{-1} I_F^0(0) \quad 12.$$

From the energy distribution of electrons at different depths various other quantities such as the rate of x-ray production, the secondary electron and Auger yield can be calculated. If x-rays with absorption coefficient  $\mu$  are produced at the rate  $\phi_i$  by electrons at energy level  $i$  and the detector makes an angle  $\theta_D$  with the specimen normal the observed rate of x-ray production would be

$$\frac{\sum \phi_i (V_{1ij} + V_{2ij}) V_{2j0}^{-1} I_F^0(0)}{\left( \lambda_j + \frac{\mu}{\cos \theta_D} \right)} \quad 13.$$

As the depth integration is analytic there is no extra effort in calculating x-ray yield as opposed to backscattering.

In calculations using this theory it was found that 10 angle elements in  $90^\circ$  were necessary for convergence at 10-15 energy intervals were needed for energy distributions of backscattered electrons. For the elastic scattering

a screened Rutherford cross section was used and for the inelastic scattering a cross section was derived from the Bethe loss law using the formula

$$\sigma(\theta_i, E_n; \theta_f, E_m) = \frac{1}{E_n - E_m} \frac{dE}{ds} \left( \frac{E_n + E_m}{2} \right) \quad 14.$$

was used.

It was found that the results were not very sensitive to small changes in screening parameter or ionization potential. However the theory is quite general and other cross sections could be used. For calculations of distribution of backscattering with atomic number and angle the single energy step theory where only absorption is considered was found to be quite adequate. Probably the most important parameter affecting backscattering is the ratio of elastic to inelastic scattering. This is illustrated in Fig. 1 which shows a plot of backscattering as a function of atomic number. The density was assumed to be  $.2342 \text{ gm cm}^{-3}$  and the mean ionization potential  $11.52 \text{ eV}$ . The agreement between calculated points and experimental points is good, the discrepancy being mainly due to the simple expressions assumed for density in the calculations. To investigate whether single large angle events are more important than many small angle events the cross section was cut off so that electrons were only scattered by  $20^\circ$  or less. Large angle events appear to be more important in light elements as the inelastic scattering is stronger and so there is less chance that electrons which have been scattered many times will leave the specimen. Fig. 2 shows the variation of backscattering with angle of incidence for 50 kV electrons. At grazing incidence the backscattering is more or less independent of atomic number. This agrees with the experiments of Kanter [7] and Monte Carlo calculations. In Fig. 3 polar plots of backscattering for 30 keV electrons at normal incidence are presented. For thin specimens the flattened distribution dominated by single scattering is apparent, for bulk specimens the distribution follows a cosine law.

The energy dissipation of 30 keV electrons for copper as a function of depth can also be calculated using this approach and this is shown in Fig. 4 with the results of Spencer's [5] calculations scaled to 30 keV. The main discrepancy is that the single energy step calculation decreases too slowly at large depths and is too low at small depths. This is to be expected as there is too much absorption of electrons near the incident energy and not enough absorption of the lower energy electrons at greater depths in the

specimen. If more energy levels are considered this can be corrected and about 5 energy levels are needed for convergence the remaining discrepancy probably being because Spencer did not use the correct boundary conditions. Similar effects due to the treatment of absorption can be seen in calculations of forward and backscattered fluxes from specimens of different thicknesses or of fluxes at various depths in a semi-infinite specimen.

In Figs. 5, 6, and 7, the energy distribution of backscattered electrons for copper, aluminum, and gold is plotted and compared with the experimental results of Darlington [10]. The agreement is good and the calculations show a broadening of the peak of the distribution with a shift in the maximum to lower energies for lower atomic number. This is a result of the ratio of inelastic to elastic scattering, the greater inelastic scattering for light elements giving rise to more energy dispersion.

One advantage of these methods over Monte Carlo calculations is the reduced computer time. For a CDC 7600 angular distributions assuming the single energy low approximation can be calculated in 0.2 sec, energy and angular distributions or x-ray production in 3 sec. and detailed energy spectra at 20 different depths in about 30 sec. This method is readily applicable to layer problems and perturbations can be easily handled. It is also possible in principle to invert the equations to calculate quantities of interest (e.g. thickness of an overlayer) from backscattering observations.

#### ACKNOWLEDGMENT

This work was supported by the U.K. Science Research Council (D.J.F. and P.R.) and the Division of Basic Energy Sciences, U.S. Department of Energy (P.R.).

#### REFERENCES

1. R. Shimizu, T. Ikuta and K. Murata, *J. Appl. Phys.* 43, 4233 (1972).
2. H.A. Bethe, M.E. Rose and L.P. Smith, *Proc. Amer. Phil. Soc.* 78, 573 (1938).
3. D.B. Brown, D.B. Wittry and D.F. Kyser, *J. Appl. Phys.* 40, 1627 (1969).
4. H.W. Lewis, *Phys. Rev.* 78, 526 (1950).
5. L.V. Spencer, *Phys. Rev.* 98, 1597 (1955).
6. J.H. Jacob, *Phys. Rev.* 8A, 226 (1973).
7. H.E. Bishop, *Proc. Phys. Soc.* 85, 855 (1965).
8. R.F. Dashen, *Phys. Rev.* 134, 1025 (1964).
9. H. Kanter, *Brit. J. Appl. Phys.* 15, 555 (1964).
10. H. Darlington, *J. Phys.* D 8, 85 (1975).

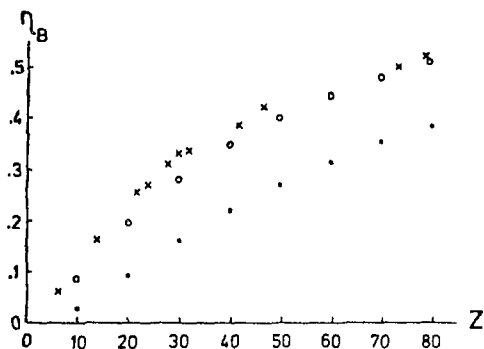


Fig. 1 Backscattered fraction  $\eta_B$  as a function of atomic number  $Z$ . The open circles 'o' are calculated points, the crosses 'x' are experimental points and the dots '.' are calculated points for scattering of  $20^\circ$  or less.

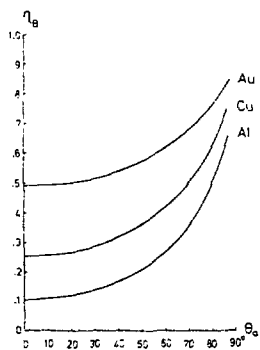


Fig. 2 Backscattered fraction  $\eta_B$  as a function of angle of incidence  $\theta_0$ .

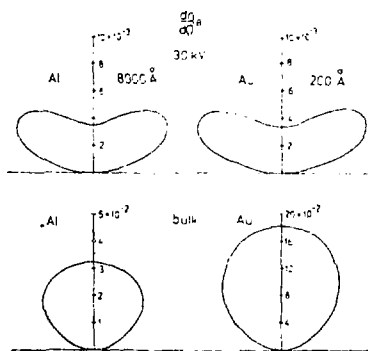


Fig. 3 Angular distributions of backscattered electrons.

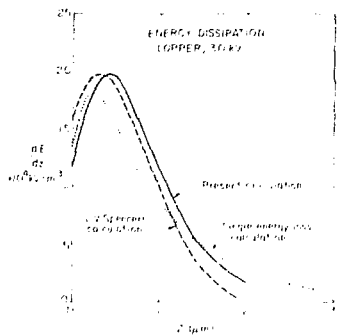


Fig. 4 Energy dissipation  $dE/dz$  as a function of depth,  $z$ , in a bulk specimen.

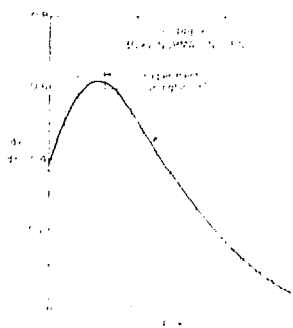


Fig. 5 Energy distribution of backscattered electrons for copper.

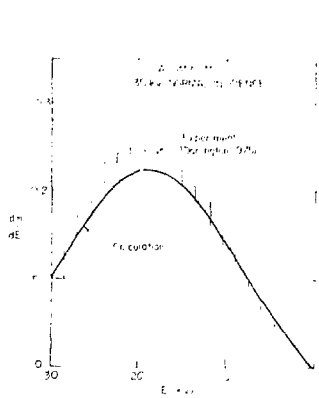


Fig. 6 Energy distribution of backscattered electrons for aluminum.

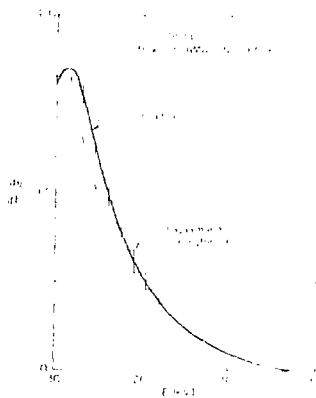


Fig. 7 Energy distribution of backscattered electrons for gold.